

# Helix Sense-Selective Supramolecular Polymerization Seeded by a One-Handed Helical Polymeric Assembly

Wei Zhang,<sup>†,‡</sup> Wusong Jin,<sup>\*,§</sup> Takanori Fukushima,<sup>\*,#</sup> Tadashi Mori,<sup>⊥</sup> and Takuzo Aida<sup>\*,†,‡</sup>

<sup>†</sup>RIKEN Center for Emergent Matter Science, 2-1 Hirosawa, Wako, Saitama 351-0198, Japan

<sup>‡</sup>Department of Chemistry and Biotechnology, School of Engineering, The University of Tokyo, 7-3-1 Hongo, Bunkyo-ku, Tokyo 113-8656, Japan

<sup>§</sup>College of Chemistry, Chemical Engineering and Biotechnology, Donghua University, 2999 North Renmin Road, Songjiang, Shanghai 201620, P. R. China

<sup>#</sup>Chemical Resources Laboratory, Tokyo Institute of Technology, 4259 Nagatsuta, Midori-ku, Yokohama 226-8503, Japan

<sup>⊥</sup>Department of Applied Chemistry, Graduate School of Engineering, Osaka University, 2-1 Yamada-oka, Suita, Osaka 565-0871, Japan

## Supporting Information

**ABSTRACT:** Helix sense-selective supramolecular polymerization was achieved using a one-handed helical nanotubular polymeric assembly as a seed. First, bipyridine (BPY)-appended achiral hexabenzocoronene (<sup>BPY</sup>HBC) was copolymerized noncovalently with chiral <sup>BPY</sup>HBC<sub>S</sub> (or <sup>BPY</sup>HBC<sub>R</sub>) at a molar ratio of 9:1, which, via the sergeants-and-soldiers effect, afforded a *P*-helical (or *M*-helical) nanotube, which was then treated with Cu<sup>2+</sup> to transform into structurally robust (<sup>BPY</sup>)CuNT<sub>(P)</sub> (or (<sup>BPY</sup>)CuNT<sub>(M)</sub>) with a Cu<sup>2+</sup>/BPY coordination polymer shell. Helical seeds (<sup>BPY</sup>)CuNT<sub>(P)</sub> and (<sup>BPY</sup>)CuNT<sub>(M)</sub> brought about the controlled assembly of fluorinated chiral FHBC<sub>S</sub> and FHBC<sub>R</sub> as well as achiral FHBC to yield one-handed helical nanotubular supramolecular block copolymers, in which the helical senses of the newly formed block segments were solely determined by those of the helical seeds employed. Noteworthy, FHBC<sub>S</sub> and FHBC<sub>R</sub> alone without the helical seeds form ill-defined agglomerates. Attempted supramolecular polymerization of a racemic mixture of FHBC<sub>S</sub> and FHBC<sub>R</sub> from (<sup>BPY</sup>)CuNT<sub>(P)</sub> (or (<sup>BPY</sup>)CuNT<sub>(M)</sub>) resulted in its chiral separation, affording *P*-helical (or *M*-helical) diastereomeric block segments composed of FHBC<sub>S</sub> and FHBC<sub>R</sub> with different thermodynamic properties.

Helicity is one of the essential structural elements in biological systems, and there is a long-standing question whether it correlates with the origin of homochirality in nature.<sup>1</sup> Starting in the 1960s, after the discovery of biological helices, the Pino group began to construct optically active synthetic polymers via the polymerization of monomers bearing chiral substituents.<sup>2</sup> In the 1970s, the Nolte and Okamoto groups reported that polymers adopting a one-handed helical conformation can be obtained from particular types of achiral monomers using chiral initiators.<sup>3</sup> Subsequently, a variety of such helical polymers and oligomers with appealing functions were synthesized using so-called “helix sense-selective polymerization”.<sup>4</sup> More recently, the synthesis of one-handed helical

block copolymers was successfully demonstrated using certain types of conformationally rigid one-handed helical polymers as macromolecular initiators.<sup>5</sup> Namely, two block segments can conformationally communicate with one another if their structures are designed to match. We began to wonder whether a helical supramolecular block copolymer has ever been synthesized. The research area of supramolecular polymerization has made remarkable progress in recent years,<sup>6</sup> and examples of living polymerization,<sup>7</sup> including the synthesis of supramolecular block copolymers, have been reported to date.<sup>7a–c,e,g,8</sup> This paradigm shift was initiated by the work of Manners et al. with the successful stepwise synthesis of block copolymer-like rod micellar aggregates from two different core-crystallizable monomers.<sup>7a</sup> This work led to some conceptual breakthroughs,<sup>7</sup> including our recent achievement of initiator-driven chain growth supramolecular polymerization.<sup>7e</sup> As exemplified by a series of studies by Meijer et al., the research history for chiral supramolecular polymerization is even longer.<sup>6,9</sup> However, regarding helix sense-selective noncovalent polymerization, no successful example has been reported. We herein demonstrate the first example of such helix sense-selective noncovalent polymerization using a molecularly engineered one-handed helical nanotubular assembly as a seed. We also highlight chiral separation of a racemic monomer in this particular block copolymerization.

The monomers we chose are Gemini-shaped hexabenzocoronene derivatives (HBC, Figure 1a). In 2004, we reported that a HBC derivative that bears two triethylene glycol-appended phenyl groups on one of its sides, and dodecyl side chains on the other side enables self-assembly into a semiconducting nanotube with inner and outer diameters of 14 and 20 nm, respectively.<sup>10</sup> The nanotube is composed of a graphite-like bilayer wall that is supported internally by the interdigitation of the dodecyl side chains and consists of helically twisted columnar arrays of  $\pi$ -stacked HBC units (Figure 1b).<sup>11</sup> The nanotube is one-handed helical, whose handedness can be controlled by the absolute configurations of the stereogenic centers, if available, in the

Received: September 20, 2015

Published: October 19, 2015

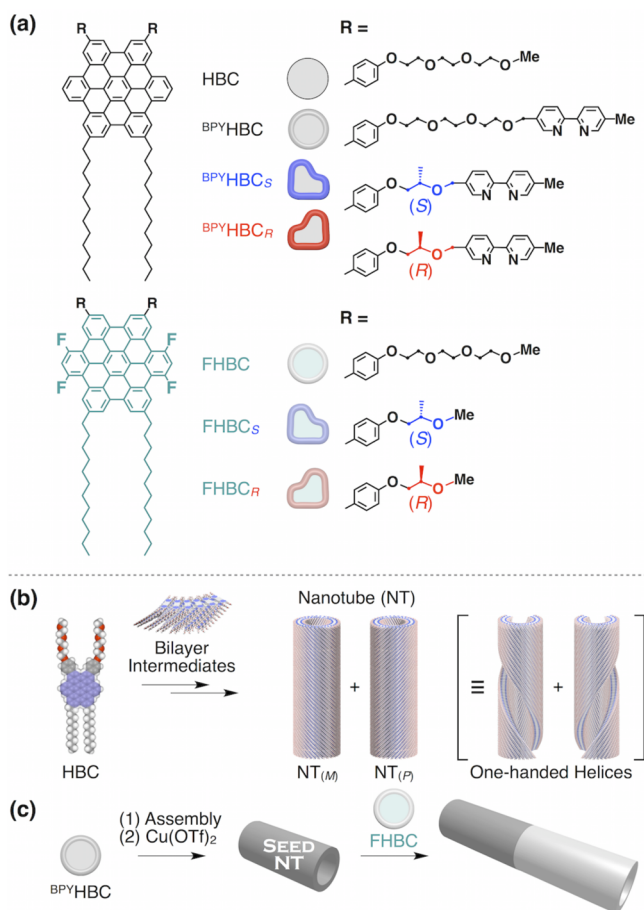


**Figure 1.** (a) Molecular structures of HBC derivatives and their logos for rapid identification. (b) Illustration of the helical chirality of the HBC nanotubes. (c) Illustration of the procedure for the formation of a nanotubular supramolecular block copolymer.

oligoether chains.<sup>12</sup> Recently, we succeeded in the synthesis of a nanotubular block copolymer by stepwise self-assembly of two strategically designed HBC motifs: <sup>BPY</sup>HBC and FHBC (Figure 1c).<sup>8</sup> <sup>BPY</sup>HBC was designed to form a structurally robust nanotube because its bipyridine units can be post-functionalized to coordinate on the nanotube surface with transition-metal ions, such as Cu<sup>2+</sup>, to form a metal–organic polymer shell (Figure 1c). FHBC was designed to stack electronically on nonfluorinated HBCs to form a stable heterojunction part in the block copolymer.<sup>8</sup>

Here, we utilized FHBC and its chiral versions, FHBC<sub>S</sub> and FHBC<sub>R</sub>, which carry stereogenic centers in their oligoether chains, as monomers (Figure 1a).<sup>13</sup> Using the ‘sergeants-and-soldiers effect’,<sup>12b,14</sup> one-handed helical seeds <sup>(BPY)Cu</sup>NT<sub>(M)</sub> and <sup>(BPY)Cu</sup>NT<sub>(P)</sub> (Figure 2) were successfully prepared via the co-assembly of <sup>BPY</sup>HBC with <sup>BPY</sup>HBC<sub>R</sub> and <sup>BPY</sup>HBC<sub>S</sub> (Figure 1a) as chiral handles. Typically, a 5 mL vial containing a CHCl<sub>3</sub> (1 mL) solution of a mixture of <sup>BPY</sup>HBC (0.135 μmol, 90 mol %) and <sup>BPY</sup>HBC<sub>S</sub> (0.015 μmol, 10 mol %) was placed into a 50 mL vial containing MeOH (10 mL) for vapor diffusion. This setup was kept at 25 °C for 48 h, wherein a yellow precipitate formed quantitatively. Transmission electron microscopy (TEM) of an air-dried sample of the suspension allowed for the visualization of bundled nanotubes (Figure S1). After the post-functionalization with Cu(OTf)<sub>2</sub> (5.0 equiv. to <sup>BPY</sup>HBC) in acetone, highly dispersed nanotubes were obtained, as observed by TEM (Figure

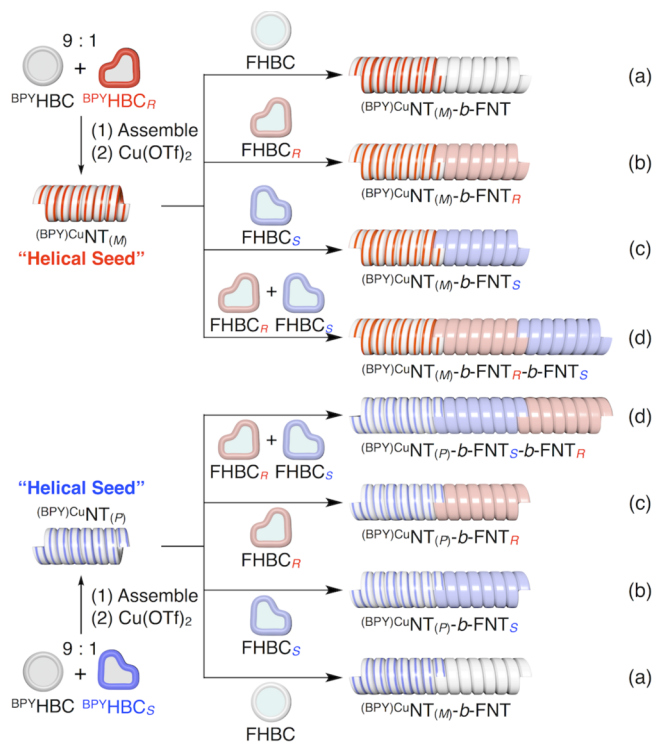


**Figure 2.** Supramolecular polymerization of FHBC, FHBC<sub>S</sub>, FHBC<sub>R</sub> and its racemic mixture seeded by <sup>(BPY)Cu</sup>NT<sub>(M)</sub> or <sup>(BPY)Cu</sup>NT<sub>(P)</sub>. For (d), a mixture of <sup>(BPY)Cu</sup>NT<sub>(P)</sub>-b-FNT<sub>S</sub> and <sup>(BPY)Cu</sup>NT<sub>(P)</sub>-b-FNT<sub>R</sub> (<sup>(BPY)Cu</sup>NT<sub>(M)</sub>-b-FNT<sub>R</sub> and <sup>(BPY)Cu</sup>NT<sub>(M)</sub>-b-FNT<sub>S</sub>) is a possible product, too.

S2) and SEM (Figure S3). The resultant acetone dispersion was active in circular dichroism (CD) spectroscopy and showed at 25 °C a positive Cotton effect centered at 430 nm with a shoulder band at 459 nm (Figure S4a, blue). As expected, when <sup>BPY</sup>HBC<sub>R</sub> was used as the co-assembling partner for <sup>BPY</sup>HBC, the resultant nanotube showed a perfect mirror-image CD spectral profile of that observed for <sup>BPY</sup>HBC<sub>S</sub> (Figure S4a, red). These Cotton effects are in a region of the absorption bands assignable to the  $\pi$ -stacked HBC units (Figure S5). When the mole fraction of <sup>BPY</sup>HBC<sub>S</sub> was increased while the total monomer concentration ( $[\text{<sup>BPY</sup>HBC}] + [\text{<sup>BPY</sup>HBC}_S]$ ) was kept constant at 0.15 mM, the CD intensity at 430 nm increased monotonically up to 8% of the mole fraction of <sup>BPY</sup>HBC<sub>S</sub> and reached a plateau (Figure S4b, blue). The same held true for the case using the opposite enantiomer <sup>BPY</sup>HBC<sub>R</sub> (Figure S4b, red). These results clearly indicate the successful operation of the ‘sergeants-and-soldiers effect’. Even under varying conditions, <sup>BPY</sup>HBC<sub>R</sub> and <sup>BPY</sup>HBC<sub>S</sub> alone do not assemble into nanotubes but ill-defined agglomerates. By chance, we found in the co-assembled mixtures (P)- and (M)-helical nanocoils as intermediates for the nanotubes, along with their parent nanotubes (Figure S6). Based on their helical handedness, we now unambiguously conclude that the co-assembly of <sup>BPY</sup>HBC with chiral <sup>BPY</sup>HBC<sub>R</sub> and <sup>BPY</sup>HBC<sub>S</sub> gives <sup>(BPY)Cu</sup>NT<sub>(M)</sub> and <sup>(BPY)Cu</sup>NT<sub>(P)</sub>, respectively.

In our previous paper, we reported that the nanotube of achiral <sup>BPY</sup>HBC with a Cu<sup>2+</sup>/BPY coordination polymer shell can serve as a seed for the nanotubular assembly of FHBC.<sup>8</sup> Prior to the main experiments using chiral FHBC<sub>R</sub> and FHBC<sub>S</sub>, we investigated whether <sup>(BPY)Cu</sup>NT<sub>(M)</sub> and <sup>(BPY)Cu</sup>NT<sub>(P)</sub>, containing 10% chiral <sup>BPY</sup>HBC<sub>R</sub> and <sup>BPY</sup>HBC<sub>S</sub>, respectively, can likewise serve as seeds for the nanotubular assembly of achiral FHBC

(Figure 2a). As a typical example, a hot mixture of FHBC and  $(\text{BPY})\text{CuNT}_{(P)}$  ( $[\text{BPY}]\text{HBC}$  (90 mol %) +  $\text{BPY}\text{HBC}_S$  (10 mol %) =  $[\text{FHBC}] = 7.5 \times 10^{-5} \text{ M}$ ) in acetone at  $65^\circ\text{C}$  was allowed to cool slowly to  $5^\circ\text{C}$ . As shown in Figure 3a,b, an air-dried sample of the

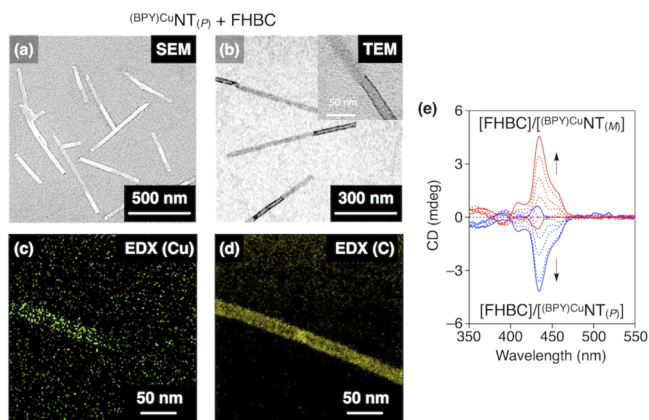


**Figure 3.** (a) SEM and (b) TEM micrographs of an air-dried acetone dispersion of  $(\text{BPY})\text{CuNT}_{(P)}\text{-b-FNT}$ . The green and yellow dots in (c) and (d) represent copper and carbon elements, respectively, in the TEM-EDX mapping of  $(\text{BPY})\text{CuNT}_{(P)}\text{-b-FNT}$ . (e) CD spectra at  $5^\circ\text{C}$  of acetone solutions of FHBC containing  $(\text{BPY})\text{CuNT}_{(P)}$  (blue) and  $(\text{BPY})\text{CuNT}_{(M)}$  (red) as seeds at  $[\text{FHBC}]/[\text{BPY}]\text{HBC}]_{\text{seed}}$  ratios of 0, 0.33, 0.67, 1.0, and 2.0.  $[\text{BPY}]\text{HBC}]_{\text{seed}} = [\text{BPY}]\text{HBC} + \text{BPY}\text{HBC}_S$  (for  $(\text{BPY})\text{CuNT}_{(P)}$ ) or  $\text{BPY}\text{HBC}_R$  (for  $(\text{BPY})\text{CuNT}_{(M)}$ ) ( $9:1$ ) $_{\text{seed}} = 7.5 \times 10^{-5} \text{ M}$ .

resultant clear dispersion exhibited micrometer-long nanotubular AB diblock and ABA triblock copolymers with bright and dark segments of a uniform diameter of  $\sim 20 \text{ nm}$  in TEM. By means of element mapping using TEM energy-dispersive X-ray spectroscopy (TEM-EDX, Figure 3c,d), we confirmed that copper is localized in the dark areas of the nanotubes in the TEM images, whereas carbon is present over the entire nanotube for all of the nanotubes. Thus,  $(\text{BPY})\text{CuNT}_{(P)}$  can serve as a seed to initiate the nanotubular supramolecular polymerization of FHBC, affording  $(\text{BPY})\text{CuNT}_{(P)}\text{-b-FNT}$  (Figure 2a). As shown in Figure 3e (blue), this nanotubular block copolymer displayed Cotton effects at 430 and 459 nm opposite to those of the seed  $(\text{BPY})\text{CuNT}_{(P)}$ . The CD bands became more intense when the amount of FHBC relative to that of the seed  $(\text{BPY})\text{CuNT}_{(P)}$  was larger. As expected, essentially the same trend was observed for the CD spectral change features when  $(\text{BPY})\text{CuNT}_{(M)}$  with an opposite handedness to  $(\text{BPY})\text{CuNT}_{(P)}$  was employed (Figure 3e, red). Theoretical calculation suggested that the energy order of the transition moments along the longer ( $x$ ) and shorter ( $y$ ) molecular axes of FHBC is opposite that of HBC (Figure S7). Thus, the chiroptical inversion observed in the polymerization of FHBC from  $(\text{BPY})\text{CuNT}_{(P)}$  or  $(\text{BPY})\text{CuNT}_{(M)}$  possibly indicates that the helical sense of the newly formed block segment is identical to that of the seed (Figure 2a).

These results prompted us to investigate how a chiral version of FHBC behaves in the polymerization.  $\text{FHBC}_S$  and  $\text{FHBC}_R$  do not undergo any defined assembly in acetone. However, when  $(\text{BPY})\text{CuNT}_{(M)}$  or  $(\text{BPY})\text{CuNT}_{(P)}$  is present as the seed, both  $\text{FHBC}_S$  and  $\text{FHBC}_R$  can be nanotubularly polymerized, regardless of the helical sense of the seed employed (Figure 2b,c). For example,  $\text{FHBC}_S$  was added to an acetone dispersion of  $(\text{BPY})\text{CuNT}_{(P)}$ , and the mixture ( $[\text{BPY}]\text{HBC}$  (90 mol %) +  $\text{BPY}\text{HBC}_S$  (10 mol %) =  $3.0 \times 10^{-4} \text{ M}$ ,  $[\text{FHBC}_S] = 6.0 \times 10^{-4} \text{ M}$ ) was heated to  $65^\circ\text{C}$  and then allowed to cool to  $5^\circ\text{C}$ . After 1 h, an aliquot was extracted

from this reaction mixture and then air-dried. Just as in the case in Figure 3a,b, this air-dried sample in SEM (Figure S8a) and TEM (Figure 4a) displayed uniform-diameter ( $\sim 20 \text{ nm}$ ) AB di- and

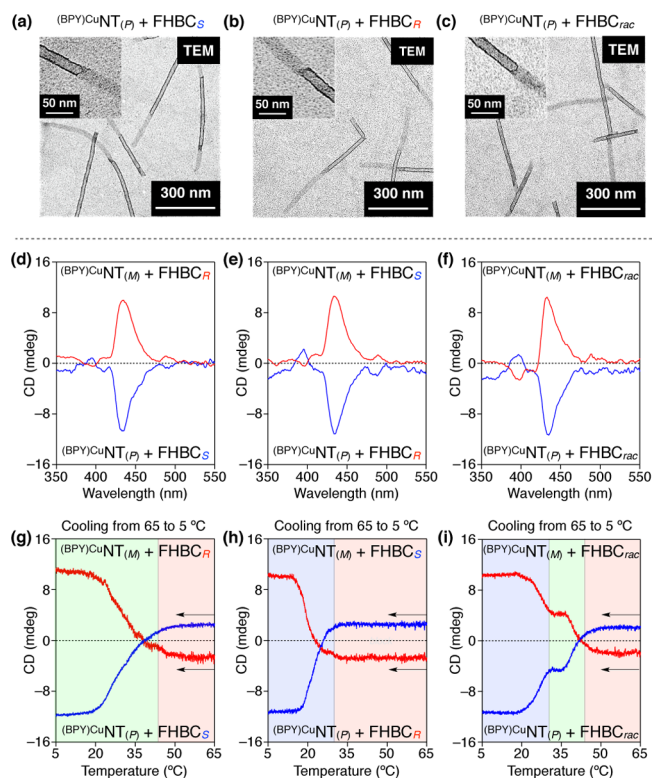


**Figure 4.** TEM micrographs of air-dried acetone dispersions of (a)  $(\text{BPY})\text{CuNT}_{(P)}\text{-b-FNT}_S$  (Figure 2b), (b)  $(\text{BPY})\text{CuNT}_{(P)}\text{-b-FNT}_R$  (Figure 2b), and (c)  $(\text{BPY})\text{CuNT}_{(P)}\text{-b-FNT}_S\text{-b-FNT}_R$  (or a mixture of  $(\text{BPY})\text{CuNT}_{(P)}\text{-b-FNT}_S$  and  $(\text{BPY})\text{CuNT}_{(P)}\text{-b-FNT}_R$ ) (Figure 2d). (d–f) CD spectra at  $5^\circ\text{C}$  of acetone dispersions of  $\text{FHBC}_S/(\text{BPY})\text{CuNT}_{(P)}$  (blue) and  $\text{FHBC}_R/(\text{BPY})\text{CuNT}_{(M)}$  (red) (d),  $\text{FHBC}_R/(\text{BPY})\text{CuNT}_{(P)}$  (blue) and  $\text{FHBC}_S/(\text{BPY})\text{CuNT}_{(M)}$  (red) (e), and  $\text{FHBC}_{\text{rac}}/(\text{BPY})\text{CuNT}_{(P)}$  (blue) and  $\text{FHBC}_{\text{rac}}/(\text{BPY})\text{CuNT}_{(M)}$  (red) (f), where  $[\text{FHBC}]/[\text{BPY}]\text{HBC}]_{\text{seed}} = 2.0$  ( $[\text{FHBC}] = [\text{FHBC}_S]$ ,  $[\text{FHBC}_R]$  or  $[\text{FHBC}_{\text{rac}}]$ ) and  $[\text{BPY}]\text{HBC}]_{\text{seed}} = [\text{BPY}]\text{HBC} + \text{BPY}\text{HBC}_S$  (for  $(\text{BPY})\text{CuNT}_{(P)}$ ) or  $\text{BPY}\text{HBC}_R$  (for  $(\text{BPY})\text{CuNT}_{(M)}$ ) ( $9:1$ ) $_{\text{seed}} = 3.0 \times 10^{-4} \text{ M}$ . (g–i) Intensity changes at 430 nm in the CD spectra (d–f) upon cooling from  $65$  to  $5^\circ\text{C}$  at a rate of  $1^\circ\text{C}/\text{min}$ .

ABA triblock nanotubular copolymers ( $(\text{BPY})\text{CuNT}_{(P)}\text{-b-FNT}_S$ ) with bright and dark segments. The same held true when  $\text{FHBC}_R$  was used instead of  $\text{FHBC}_S$  ( $(\text{BPY})\text{CuNT}_{(P)}\text{-b-FNT}_R$ , Figures S8b and 4b). Likewise, left-handed  $(\text{BPY})\text{CuNT}_{(M)}$  was able to seed the block copolymerization of  $\text{FHBC}_S$  and  $\text{FHBC}_R$  to give  $(\text{BPY})\text{CuNT}_{(M)}\text{-b-FNT}_S$  and  $(\text{BPY})\text{CuNT}_{(M)}\text{-b-FNT}_R$ , respectively (Figures S9 and S10). Figure 4d (blue) and 4e (blue) shows the CD spectra of  $(\text{BPY})\text{CuNT}_{(P)}\text{-b-FNT}_S$  and  $(\text{BPY})\text{CuNT}_{(P)}\text{-b-FNT}_R$ , respectively, in acetone at  $5^\circ\text{C}$ . Even though the monomers for the newly formed block segments are antipodal to one another, these CD spectra are essentially the same, with a negative Cotton effect at 430 nm. When  $(\text{BPY})\text{CuNT}_{(M)}$  with an opposite handedness to  $(\text{BPY})\text{CuNT}_{(P)}$  was used as the seed, products  $(\text{BPY})\text{CuNT}_{(M)}\text{-b-FNT}_R$  (Figure 4d, red) and  $(\text{BPY})\text{CuNT}_{(M)}\text{-b-FNT}_S$  (Figure 4e, red) both exhibited a positive Cotton effect at 430 nm. Specifically, as in the case of achiral FHBC, the helical sense of the seed determines those of the seeded segments  $\text{FNT}_S$  and  $\text{FNT}_R$  in the products (Figure 2b,c). Note that the left-handed (or right-handed)  $\text{FNT}_S$  and  $\text{FNT}_R$  segments should be diastereoisomeric to one another, and their

thermodynamic properties differ accordingly. Because the Cotton effect at 430 nm originates from the J-aggregated HBC units, it is usable as a probe for evaluating the thermal stability of the NTs. Figure 4g (blue) shows the CD intensity change of an acetone dispersion of  $(\text{BPY})\text{CuNT}_{(P)}\text{-}b\text{-FNT}_S$  at 430 nm upon cooling from 65 to 5 °C at a rate of 1 °C/min. This thermal profile exhibited a sigmoidal increase in CD intensity after an initial plateau region, displaying a transition point at ~43 °C, where FHBC<sub>S</sub> likely starts to self-assemble at the edge parts of the seed, affording a right-handed nanotubular segment. As expected, its enantiomer  $(\text{BPY})\text{CuNT}_{(M)}\text{-}b\text{-FNT}_R$  showed exactly the same thermal profile (Figure 4g, red) as  $(\text{BPY})\text{CuNT}_{(P)}\text{-}b\text{-FNT}_S$ , while  $(\text{BPY})\text{CuNT}_{(P)}\text{-}b\text{-FNT}_R$ , a diastereoisomer to  $(\text{BPY})\text{CuNT}_{(P)}\text{-}b\text{-FNT}_S$ , showed a different thermal profile displaying a transition temperature at 27 °C (Figure 4h, blue). The same temperature-dependent spectral trends were observed for  $(\text{BPY})\text{CuNT}_{(M)}\text{-}b\text{-FNT}_S$  (Figure 4h, red).

Based on these results, we investigated the assembly upon mixing racemic FHBC<sub>rac</sub> with helical seed  $(\text{BPY})\text{CuNT}_{(P)}$  or  $(\text{BPY})\text{CuNT}_{(M)}$  (Figure 2d). TEM and SEM (Figures 4c, S11, and S12) showed the formation of well-defined nanotubular block copolymers. As expected, the CD spectral features of the resulting products (Figure 4f) are analogous to those observed in Figure 4d,e, where the block copolymers seeded by  $(\text{BPY})\text{CuNT}_{(P)}$  and  $(\text{BPY})\text{CuNT}_{(M)}$  show negative (blue) and positive (red) Cotton effects at 430 nm, respectively. Next, we investigated their CD intensity changes at 430 nm upon cooling from 65 to 5 °C. Of particular interest, in both cases, we observed two distinct transition behaviors at around 43 and 27 °C in Figure 4i. Noteworthy, the former and latter transition points are identical to those separately observed in Figure 4g,h, respectively. This observation indicates that FHBC<sub>R</sub> and FHBC<sub>S</sub> homochirally polymerize (chiral separation) from the edge parts of the helical seed (Figure 2d), although it is difficult to distinguish whether the product is  $(\text{BPY})\text{CuNT}_{(P)}\text{-}b\text{-FNT}_S\text{-}b\text{-FNT}_R$  ( $(\text{BPY})\text{CuNT}_{(M)}\text{-}b\text{-FNT}_R\text{-}b\text{-FNT}_S$ ) or a mixture of  $(\text{BPY})\text{CuNT}_{(P)}\text{-}b\text{-FNT}_S$  and  $(\text{BPY})\text{CuNT}_{(P)}\text{-}b\text{-FNT}_R$  (a mixture of  $(\text{BPY})\text{CuNT}_{(M)}\text{-}b\text{-FNT}_R$  and  $(\text{BPY})\text{CuNT}_{(M)}\text{-}b\text{-FNT}_S$ ).

Despite recent breakthroughs in supramolecular polymerization,<sup>6–9</sup> there still exists a strong preconceived notion that supramolecular polymers are too dynamic to construct in a sequence-specific manner. This notion might be true, but it is not always the case. The unprecedented achievements made in the present work fill a knowledge gap between covalent and supramolecular polymerizations.

## ■ ASSOCIATED CONTENT

### Supporting Information

The Supporting Information is available free of charge on the ACS Publications website at DOI: 10.1021/jacs.5b09878.

Details of the experimental procedures, electron micrographs, absorption spectra, and synthesis of all compounds (PDF)

## ■ AUTHOR INFORMATION

### Corresponding Authors

\*wsjin@dhu.edu.cn

\*fukushima@res.titech.ac.jp

\*aida@macro.t.u-tokyo.ac.jp

### Notes

The authors declare no competing financial interest.

## ■ ACKNOWLEDGMENTS

This work was supported by the Japan Society for the Promotion of Science (JSPS) through its Grant-in-Aid for Specially Promoted Research (25000005) on “Physically Perturbed Assembly for Tailoring High-Performance Soft Materials with Controlled Macroscopic Structural Anisotropy”.

## ■ REFERENCES

- (1) (a) Bonner, W. A. *Origins Life Evol. Biospheres* **1991**, *21*, 59. (b) Weissbuch, I.; Leiserowitz, L.; Lahav, M. *Top. Curr. Chem.* **2005**, *259*, 123.
- (2) Pino, P.; Lorenzi, G. P. *J. Am. Chem. Soc.* **1960**, *82*, 4745.
- (3) (a) Nolte, R. J. M.; Van Beijnen, A. J. M.; Drenth, W. *J. Am. Chem. Soc.* **1974**, *96*, 5932. (b) Okamoto, Y.; Suzuki, K.; Ohta, K.; Hatada, K.; Yuki, H. *J. Am. Chem. Soc.* **1979**, *101*, 4763.
- (4) For reviews: (a) Okamoto, Y.; Nakano, T. *Chem. Rev.* **1994**, *94*, 349. (b) Nolte, R. J. M. *Chem. Soc. Rev.* **1994**, *23*, 11. (c) Green, M. M.; Peterson, N. C.; Sato, T.; Teramoto, A.; Cook, R.; Lifson, S. *Science* **1995**, *268*, 1860. (d) Nakano, T.; Okamoto, Y. *Chem. Rev.* **2001**, *101*, 4013. (e) Cornelissen, J. J. L. M.; Rowan, A. E.; Nolte, R. J. M.; Sommerdijk, N. A. J. M. *Chem. Rev.* **2001**, *101*, 4039. (f) Lam, J. W. Y.; Tang, B. Z. *Acc. Chem. Res.* **2005**, *38*, 745. (g) Pijper, D.; Feringa, B. L. *Soft Matter* **2008**, *4*, 1349. (h) Yashima, E.; Maeda, K.; Iida, H.; Furusho, Y.; Nagai, K. *Chem. Rev.* **2009**, *109*, 6102.
- (5) (a) Ito, Y.; Ihara, E.; Murakami, M. *Angew. Chem., Int. Ed. Engl.* **1992**, *31*, 1509. (b) Takei, F.; Yanai, K.; Onitsuka, K.; Takahashi, S. *Angew. Chem., Int. Ed. Engl.* **1996**, *35*, 1554. (c) Takei, F.; Yanai, K.; Onitsuka, K.; Takahashi, S. *Chem. - Eur. J.* **2000**, *6*, 983. (d) Sugimoto, M.; Collet, S.; Ito, Y. *Org. Lett.* **2002**, *4*, 351. (e) Wu, Z.-Q.; Nagai, K.; Banno, M.; Okoshi, K.; Onitsuka, K.; Yashima, E. *J. Am. Chem. Soc.* **2009**, *131*, 6708.
- (6) (a) Brunsveld, L.; Folmer, B. J. B.; Meijer, E. W.; Sijbesma, R. P. *Chem. Rev.* **2001**, *101*, 4071. (b) De Greef, T. F. A.; Smulders, M. M. J.; Wolfs, M.; Schenning, A. P. H. J.; Sijbesma, R. P.; Meijer, E. W. *Chem. Rev.* **2009**, *109*, 5687. (c) Aida, T.; Meijer, E. W.; Stupp, S. I. *Science* **2012**, *335*, 813.
- (7) (a) Wang, X.; Guerin, G.; Wang, H.; Wang, Y.; Manners, I.; Winnik, M. A. *Science* **2007**, *317*, 644. (b) Rupar, P. A.; Chabanne, L.; Winnik, M. A.; Manners, I. *Science* **2012**, *337*, 559. (c) Hudson, Z. M.; Lunn, D. J.; Winnik, M. A.; Manners, I. *Nat. Commun.* **2014**, *5*, 4372. (d) Ogi, S.; Sugiyasu, K.; Manna, S.; Samitsu, S.; Takeuchi, M. *Nat. Chem.* **2014**, *6*, 188. (e) Kang, J.; Miyajima, D.; Mori, T.; Inoue, Y.; Itoh, Y.; Aida, T. *Science* **2015**, *347*, 646. (f) Ogi, S.; Stepanenko, V.; Sugiyasu, K.; Takeuchi, M.; Würthner, F. *J. Am. Chem. Soc.* **2015**, *137*, 3300. (g) Qiu, H.; Hudson, Z. M.; Winnik, M. A.; Manners, I. *Science* **2015**, *347*, 1329.
- (8) Zhang, W.; Jin, W.; Fukushima, T.; Saeki, A.; Seki, S.; Aida, T. *Science* **2011**, *334*, 340.
- (9) (a) Jonkheijm, P.; van der Schoot, P.; Schenning, A. P. H. J.; Meijer, E. W. *Science* **2006**, *313*, 80. (b) Korevaar, P. A.; George, S. J.; Markvoort, A. J.; Smulders, M. M. J.; Hilbers, P. A. J.; Schenning, A. P. H. J.; De Greef, T. F. A.; Meijer, E. W. *Nature* **2012**, *481*, 492. (c) Baker, M. B.; Albertazzi, L.; Voets, I. K.; Leenders, C. M. A.; Palmans, A. R. A.; Pavan, G. M.; Meijer, E. W. *Nat. Commun.* **2015**, *6*, 6234.
- (10) Hill, J. P.; Jin, W.; Kosaka, A.; Fukushima, T.; Ichihara, H.; Shimomura, T.; Ito, K.; Hashizume, T.; Ishii, N.; Aida, T. *Science* **2004**, *304*, 1481.
- (11) Jin, W.; Yamamoto, Y.; Fukushima, T.; Ishii, N.; Kim, J.; Kato, K.; Takata, M.; Aida, T. *J. Am. Chem. Soc.* **2008**, *130*, 9434.
- (12) (a) Jin, W.; Fukushima, T.; Niki, M.; Kosaka, A.; Ishii, N.; Aida, T. *Proc. Natl. Acad. Sci. U. S. A.* **2005**, *102*, 10801. (b) Yamamoto, T.; Fukushima, T.; Kosaka, A.; Jin, W.; Yamamoto, Y.; Ishii, N.; Aida, T. *Angew. Chem., Int. Ed.* **2008**, *47*, 1672.
- (13) See Supporting Information.
- (14) Green, M. M.; Reidy, M. P. *J. Am. Chem. Soc.* **1989**, *111*, 6452.